RSC Advances

ROYAL SOCIETY OF CHEMISTRY

www.rsc.org/advances

TITLE:

Intra-Articular Delivery of Methotrexate loaded Nanostructured Lipid Carrier Based Smart Gel for Effective treatment of Rheumatic Diseases

AUTHORS:

Chetan G. Shinde[1], T.M. Pramod kumar[1], M.P. Venkatesh[1]*, K.S. Rajesh[2], Atul Srivastava[1], Riyaz Ali M. Osmani[1] and Yogesh H. Sonawane[3]

[1]Dept. of Pharmaceutics, JSS University, JSS College of Pharmacy, SS Nagara, Mysore-15, Karnataka, India

[2]Dept. of Pharmaceutics, Oxbridge College of Pharmacy, Magadi main road, Bangalore-91, Karnataka, India

[3]Dept. of Pharmaceutics, MVP Samaj College of Pharmacy, Gangapur road, Nashik-02, Maharashtra, India

***CORRESPONDING AUTHOR:**

Dr. M.P. Venkatesh
Assistant Professor
Department of Pharmaceutics
JSS College of Pharmacy, Mysore-570015
Karnataka, India
E-mail address: venkateshmpv22@gmail.com
Tel.: +91 9480405487, Fax: 0821-2548359

ABSTRACT

Nanostructured lipid carrier (NLC) based smart gel of Methotrexate (MTX) was developed as potential system for the treatment of rheumatic diseases (RD). NLC composed of compritol ATO 888 as solid lipid, Capmul MCM EP as liquid lipid, Tween 80 as surfactant and PEG 400 as co-surfactant, was prepared by modified hot homogenization followed by melt ultrasonication. Characterization of the prepared NLC dispersion was assessed by means of particle size analysis, polydispersity index (PDI), entrapment efficiency and zeta potential. The nanoparticulate dispersion was suitably gelled into the polymer matrix of Pluronic F-127 (PF-127) and Pluronic F-68 (PF-68). Two-factor three-level full factorial design was employed to determine the optimum concentration of PF-127 and PF-68. The prepared NLC based smart gel was evaluated for viscosity, sterility, thermosensitivity, syringeability, content uniformity and *in vitro* release behaviour. The efficacy and biocompatibility of NLC based smart gel were established using adjuvant arthritis model and histology analysis respectively. The average particle size of NLC was 107 ± 6 nm, PDI of 0.365 ± 0.03, entrapment efficiency of 69.53 ± 1.23% and zeta potential of -13.54 ± 1.1mV. The optimized NLC based smart gel (F-10) was found to be thermo-sensitive and exhibited drug release of 92.41% at 108 h. The results demonstrated that MTX was evenly distributed in the optimized formulation, which was sterile and syringeable through 18 gauze needle. A significant decrease in rat joint swelling was observed using MTX-NLC based gel during a 28 day period. In conclusion, MTX-NLC based gel could be a potential formulation for intra-articular treatment of inflammation in rheumatic conditions.

Keywords: Methotrexate; Nanostructured lipid carrier; Intra-articular delivery; Rheumatic diseases

1. INTRODUCTION

The classical Indian medicine text *Charaka Samhita* gave the most former descriptions of rheumatic diseases (RD) as a condition with pain and swollen joints. RD are the debilitating diseases characterized by pain, inflammation of joints, with proliferation of synovium and progressive erosion of cartilage and bone; which ultimately results into the functional disability and affects overall quality of life[1,2]. Rheumatoid arthritis (RA) and Osteoarthritis (OA) are rheumatic diseases with unknown etiology, in which RA is chronic inflammatory condition while OA is mainly progressive degenerative disease. Unlike RA, OA is a relatively non-inflammatory condition, although limited synovitis can be observed[3].The average age of persons with RA is 66.8 years[4]; while OA is the most common form of arthritis in the United States with a monetary treatment cost of $8 billion[5].

Despite extended pharmaceutical and clinical research, there is no curative treatment available for the RD. Therefore, the management is achieved by various anti-rheumatic drugs; however, oral and systemic administration of such drugs is hampered by numerous adverse drug reaction and serious toxicities[6]. Nonsteroidal anti-inflammatory drugs, glucocorticoids, disease-modifying anti-rheumatic drugs (DMARDs) and biologicals have been widely used alone or in combination to restrain RD activity without complete suppression of the same. As curative treatments of RD are still unavailable, its management is made by various DMARDs such as Methotrexate (MTX).

In the current era of biological targeted therapies, MTX (Fig. 1) remains the initial preferred anti-rheumatic drug and is considered to be a gold standard treatment for RA[7]. Recent clinical findings have proved that MTX can also be used for the management of OA. MTX has a dual effect of immunosuppressant and anti-inflammatory, which can be helpful in

RD[8, 9]. However, poor pharmacokinetics and narrow safety margin of MTX limit its therapeutic benefits as conventional delivery. Treatment using MTX is discontinued in 8-19% patients due to diverse drug-related toxicities, including suppression of the formation of new blood cells leading to a severe form of anaemia, liver damage, pulmonary disturbances, renal disturbances, gastrointestinal disturbances and may leads to affect central nervous system[10].

There is a lack of clear clinical recommendations/ universally accepted regimens for use of MTX in patients with RD because of variability and unpredictability of the pharmacological action with relatively high toxicity. Therefore, rheumatologists have a considerable variability regarding MTX starting dosage, dosage increment size, interval between increments, and the route of administration[11]. These physicochemical and biological characteristics make MTX a challenge for formulation scientist to develop safe and efficacious drug delivery system. To circumvent the various drug-related toxicities of MTX, there is an urgent need for the advanced dosage form which ensures bioavailable MTX concentration at the target site i.e. intra articular (IA) with a less exposure to other body tissues. Therefore, development of new injectable IA drug delivery systems has received remarkable attention over the past few years.

IA administration of the dosage form will give a site specific delivery of a drug to the rheumatic joints, which offers possibility of avoiding various drug related toxicities, because of the availability of maximum concentration of drug at the site of action[3]. Nevertheless, rapid clearance of the drug from the joints is a major issue in the IA delivery systems; consequently there is a need for multiple injections; which can lead to infection or joint disability[12]. An innovative way to resolve this issue is by administration of depot formulation which can maintain therapeutic concentration of drug for long period of time. A significant drawback of the depot formulations upon IA injection can generate inflammatory conditions which lead to

crystal-induced arthritis[13-17]. Crystal induced pain/arthritis might depend on size and bio incompatibility of the dosage form introduced in the joint cavity[18].

Among the array of available nanoparticle based dosage forms, lipid-based nano carriers have taken the lead because of their evident benefits of higher degree of biocompatibility and versatility. The proven efficacy and safety of lipid-based carriers make them attractive candidates for topical, oral, pulmonary or parenteral delivery. These systems can be tailored, which makes them commercially viable to meet a wide range of drug delivery requirements demanded by disease conditions, routes of administration, safety and efficacy, stability and cost[19]. Nanostructured lipid carriers (NLCs) are lipid colloidal carrier system, characterized by a solid lipid matrix consisting of a mixture of liquid and solid lipids, with an average particle diameter in nanometer range. NLCs system overcome the potential limitations of solid lipid nanoparticle (SLN) such as low payload, drug expulsion during storage and high water content of SLN dispersions. Thus, they are proposed as the second generation of SLN with a special nanostructure. NLCs, due to their nanosize and solid lipid matrix, penetrate into mucosa or skin to give a controlled release of drug for a long period of time. This becomes an important tool to reduce systemic toxicity and irritation produced by the drug[20].

Polymeric smart gels that undergo sol-gel transaction in physiological temperature have shown number of applications in drug delivery. At physiological conditions, polymer conformation changes from sol-gel forming depot, which releases the drug in controlled manner. These systems can be easily formulated, sterilized and delivered at specific site of action in the body and has long retention time because of gel formation. They can be tailored to reduce systemic side effects by reducing the drug required for therapeutic effect by dose adjustment, thereby improving patient compliance and comfort. Pluronic F-127 (PF-127) and Pluronic F-68

(PF-68) are thermosensitive, biocompatible and biodegradable polymer that are generally regarded as non-toxic and non-irritant material. Also, they are listed in FDA's inactive ingredient database[21, 22].

Ultimately, the main objective of treatment in RD is to reduce joint inflammation, pain and functional restoration of the same to prevent destruction, deformity and long term disability of patients. So there is a need for the delivery system which gives faster onset yet optimum prolongs localised drug release. Taking this into account, all the positives of NLC and polymeric smart gels, formulation of NLC based smart gel system was chosen. In our present study, we experimented the direct delivery of MTX to the intra articular cavity by formulating biodegradable, injectable novel MTX NLC based smart gel for prolong release of MTX in effective treatment of rheumatic diseases and related conditions.

2. MATERIALS AND METHODS

2.1. Materials

MTX (purity >98%) was kindly provided as a gift sample from Lupin Pharma, Mumbai, India; Capmul MCM (glyceryl mono-dicaprylate) from Abitech Corporation through Indchem International, Mumbai, India. Compritol ATO 888 (glyceryldibehenate, m.p. 69-74 ºC) was donated by Gattefosse France through Colorcon Asia Pvt. Ltd., Mumbai, India. Tween 80 [$C_{32}H_{60}O_{10}$] and PEG 400 [$HO(C_2H_4O)_nH$] were purchased from SD Fine Chemicals, Mumbai, India. Pluronic F-127 (PF-127), Pluronic F-68 (PF-68), mBSA (methylated bovine serum albumin) and Freund's complete adjuvant were purchased from Sigma-Aldrich, St. Louis, USA. All other chemicals and reagents used were of analytical grade. Doubly distilled water was used for all experiments.

2.2 Methods

2.2.1. MTX assay

The quantitative determination of MTX was performed by ultra-fast liquid chromatography (UFLC-LC-20AD, Shimadzu, Kyoto, Japan). The assay was performed on a reverse phase Kromasil-C18 column (inner diameter 250 mm x 4.6 mm, pore size 5µ). The mobile phase was a mixture of 0.01N sodium acetate buffer and acetonitrile 70:30 (v/v). The injection volume was 10 µl at flow rate of 1.0 mL/min. The column effluent was detected at 307 nm with a PDA detector[23].

2.2.2. Formulation of NLC

The NLCs were prepared by a modified method of hot homogenization followed by melt ultrasonication[24]. The lipids Capmul MCM EP (liquid lipid) and Compritol ATO 888 (solid lipid) in 1:2 ratio (w/w), surfactant Tween 80 and PEG 400 in 2:1 (w/w) ratio were used in the formulation of NLCs. Both the lipids were mixed and melted at 75 ºC along with MTX. Molten lipid phase was dispersed into a preheated (75 ºC) aqueous Tween 80-PEG 400 solution, under continuous stirring with the aid of agitation at 600 rpm for 10 min and the combination was immediately mixed with a hot homogenizer (Polytron® PT 1600E) at 2000 rpm for 10 min. The formed dispersion was subjected to ultrasonication for 5 min at 70% regulable frequency, repeated four times with an interval of 10 s to reduce particle size to nanometer range using a probe type sonicator (Vibra-Cell™, Sonics and Materials, Inc, Newtown, CT, USA). The formulations were cooled down to room temperature and were stored in light-protected sealed containers at 4°C.

2.2.3. Formulation of NLC based smart gels

NLC-embedded smart gel was prepared to increase viscosity and improve localization of depot in IA Cavity. PF-127 and PF-68 served as gelling agents and were dispersed in NLC aqueous dispersion directly. Smart gel of polymers were prepared according to the so-called "cold method"[25]. The MTX-NLC based smart gel was prepared by adding Pluronic F-127 (20-24 % w/w) and Pluronic F-68 (2-6 % w/w) polymers directly into NLC dispersion and cooling it overnight at 4 °C. Direct addition of polymers instead of a preformed smart gel avoids drug dilution. pH of the final formulation was adjusted to neutral using triethanolamine. Benzalkonium chloride (0.001 % w/v) was added to the gel as a preservative. The prepared gels were packed in amber color glass vials and sealed for further use.

2.2.4. Experimental design

Experimental design is a systematic and scientific approach to study the relationship and interaction between independent and dependent variables. A 2-factor, 3-level full factorial design (3^2) was employed for optimizing NLC based smart gels using DESIGN EXPERT® (version 9.0.5) software available from Stat-Ease Inc., Minneapolis, MN. The concentration of PF-127(A) and PF-68 (B) were optimized by using Design of Experiment (DoE) at three different levels: low (-1), medium (0) and high (+1). Gelation temperature (°C) (R1); Gelation time (sec) (R2); syringeability test (sec) (R3); *in vitro* drug release studies (% cumulative drug release) (R4) were selected as response variables. A statistical model incorporating interactive and polynomial terms was utilized to evaluate the formulation responses; Eq. (1).

$$Y=b_0+ b_1A+b_2B+ b_3AB+ b_4A^2 +b_5B^2 \qquad (1)$$

Where, Y is the response, b_0 is the arithmetic mean response of the 9 runs. The responses in the above equation Y are the quantitative effect of formulation components or independent variables A and B; b_0 is the arithmetic mean response; b_1, b_2, b_3, b_4 and b_5 are the estimated co-efficient for the factors A and B. Details of the factorial design are given in the Table 1. The prepared NLC based smart gels were characterised and evaluated for sol-gel transition, syringeability, *in vitro* drug release studies, uniformity of drug content and viscosity studies.

2.2.5. Characterization of NLC

The prepared NLC were characterized and evaluated for particle size, zeta potential, polydispersity index (PDI), scanning electron microscopy (SEM), entrapment efficiency and drug loading.

2.2.5.1. Particle size, Zeta potential measurement

Samples were diluted to 1:10000 ratio with distilled water and mean particle size, poly dispersity index and zeta potential were determined by dynamic light scattering (DLS) using particle size analyzer (Zetasizer 3000, Malvern Instruments Worcestershire, UK) at a scattering angle of 90°. All measurements were carried out in triplicate under ambient conditions.

2.2.5.2. Scanning electron microscopy

The surface morphology of the optimized NLCs was observed using scanning electron microscope (Hitachi Ltd., S-3400N type II model, Tokyo, Japan). Samples were mounted on carbon mount using double-sided adhesive tape and were scanned at an accelerating voltage of 15 KV.

2.2.5.3. Entrapment efficiency and drug loading

Determination of the amount of drug incorporated in NLC is of prime importance, since it influences the release characteristics. The amount of drug encapsulated per unit weight of the nanoparticles is determined after separation of the free drug and solid lipids from the aqueous medium by centrifugation at 10,000 rpm. Prepared NLC containing drug equivalent to one dose was added in 50 mL volumetric flask containing methanol at 75°C and centrifuged for 20 min at 10,000 rpm. The supernatant solution was suitably diluted and analyzed for drug content using UFLC at 307 nm. The drug entrapment efficiency[26] (EE) and drug loading[27] (DL) in the NLCs was calculated by the following equation. All measurements were carried out in triplicates under ambient conditions.

$$EE = (Wa\text{-}Ws / Wa) \times 100 \quad (2)$$

$$DL = (Wa\text{-}Ws / W_I) \times 100 \quad (3)$$

Where, Wa is total weight of drug added to formulation, Ws is analyzed weight of drug from supernatant and W_I is total weight of lipids

2.2.6. Characterization of NLC based Smart gel

2.2.6.1. Gelation temperature

The gelation temperature of NLC based smart gel was estimated by heating the solution in a thin walled glass tube (internal diameter-10 mm, length-82 mm, thickness-0.6 mm) placed in a temperature controlled water bath with gentle shaking till it is converted to gel. The temperature of water was increased at a rate of 2 °C/5 min constantly. Gel formation was taken as the point where there was no flow when the test tube was overturned. This temperature was noted as gelation temperature[22].

2.2.6.2. Gelation time

Gelation time of NLC based smart gel was determined by tube inverting method. 2 mL of in situ gel taken in a thin-walled glass tube was immersed at the respective gelation temperature in a temperature-controlled water bath. The test tube was taken out at regular intervals and inverted to observe physical state of the sample. The gelation time was determined by a flow or no-flow criterion with the test tube inverted. Time taken for the system to gel was noted[22].

2.2.6.3. Syringeability test

Syringeability test was performed according to the method described by Yannic *et al*., [28]. Syringeability of gels was evaluated with a device composed of vertical support for a 5.0 ml glass syringe (18G needle) filled with smart gel maintained at 5±1°C and a pan resting on the piston of the syringe. The average time required to expel 5 mL of formulation under constant pressure (0.5 kg mass) was recorded as the syringeability time.

2.2.6.4. In vitro drug release study

The MTX loaded NLC (MTX-NLC) based smart gels were dispersed in 10 mL of pH 7.4 phosphate buffer solution in a sealed jacketed beaker at 37±0.5°C. The assembly was shaken continuously at 60 rpm at 37±0.5°C using a shaker (Yamato, Japan) [29]. Aliquots of 1 ml were withdrawn at regular intervals and replaced by an equal volume of fresh warm medium using syringe needle. The amount of drug released was analysed using UFLC at 307 nm.

2.2.6.5. Drug content

1 ml of NLC based smart gel was dissolved in pH 7.4 phosphate buffer and diluted up to 100 ml. Drug content was evaluated by measuring the absorbance at 307 nm in UFLC[30, 31].

2.2.6.6. Viscosity studies

The viscosity measurements of the formulated NLC based smart gels were carried out using Brookfield viscometer (Brookfield DV Pro-II, United States) with spindle No. 5 at a speed of 50 rpm. The viscosity was measured (n=3) at two temperatures viz. 8 ± 1°C and at 37 ± 1ºC using a thermo stated water jacket. The samples were equilibrated for 10 min before the measurement; also the instrument was equipped with a temperature control unit[32, 33].

2.2.7. Sterilization and sterility testing

The optimized formulation was sealed in a nitrogen atmosphere and irradiated by gamma rays from a Cobalt-60 chamber to obtain 15.76 kGy final dose (Microtrol, Bangalore, India). The sterilized formulation was immersed in a Mueller-Hinton broth (Titan Biotech Ltd., Delhi, India) for cultivation of microorganisms and maintained under agitation at 37°C for 5 days. Sterile broth was used as negative control, while unsterilized gel was used as positive control. Clouding of the broth indicates contamination and inefficient sterilization, while a clear and uncontaminated broth indicates efficient sterilization[34].

2.2.8. *In vivo* study

Animal models of arthritis with a proven track record of predictability include the rat adjuvant arthritis model. It is widely used polyarthritis model for preclinical testing of numerous anti-arthritic agents[35]. Experimental procedures were performed in accordance with the ethical guidelines for the study and were approved by the Institutional Animal Ethical Committee, JSS College of pharmacy, JSS University, Mysore (Proposal No. 160/2014). A total of 18 male Wistar rats (150-200 g, 6-8 weeks) were used. Induction of chronic arthritis was done on two instances 7 days apart with an emulsion of equal volumes of mBSA in Freund's complete

adjuvant given subcutaneously in the flank (0.5ml). On 14th day of immunization the rats were given intra-articular injections: mBSA (0.5 mg in 50 µl saline) and 50 µl saline into the same knee under halothane/oxygen anaesthesia. The development of arthritis was monitored at regular intervals by measuring circumference of the right knee joint using a flexible tape meter. On day 14, the animals were randomized in different treatment group viz. control and test. Each animal received an IA injection into the right knee joint of either 100 µL of MTX solution in PBS (free MTX) or 100 µL of MTX-NLC based smart gel or 100 µL of saline (0.9% w/v). After the IA injections of developed smart gel formulation, the animals were observed at regular intervals for swelling of joints. To avoid bias, the treatment group assignments were blinded for the investigators[36, 37].

2.2.9. Biocompatibility assessment

Biocompatibility assessment of developed formulation to the synovium was done by histopathological studies using Male Wistar rats (150-200 g, 6-8 weeks). The MTX-NLC based smart gel was injected into the right knee joint (100 µL) and saline solution (100 µL) was injected into the left knee joint as control. Till day 7, the swelling in joints was monitored, and then the rats were euthanized and joints were isolated. The joints were placed in 10% formalin for 48 h, dehydrated serially, paraffin-embedded and stained with haematoxylin and eosin. Samples were examined by light microscope (Olympus BX 51: Olympus, Tokyo, Japan) by an expert pathologist to monitor the tissue reactions and cell infiltration in the synovium[38].

3. RESULT AND DISCUSSION

3.1. Preparation of MTX-NLC and NLC based smart gel

The preparation of NLC involved two main steps; (i) preparation of uniform dispersion of

drug in a suitable base, (ii) reduction of particle size. The oil phase consists of Capmul MCM EP-Compritol 888 ATO in the ratio of 1:1, Tween 80 and PEG 400 (at 2:1) as surfactant and co-surfactant. The NLC formulations were prepared by a modified method of hot homogenization followed by melt ultrasonication. This modified method mainly used to reduce globule size of the formed dispersion in the nanometer range[39]. A similar phenomenon was reported during the formulation of fenofibrate loaded NLC for oral bioavailability enhancement[40]. Plain NLC formulation showed translucent nature with a bluish tinge, while the obtained MTX-NLC formulations existed as milky dispersion with off-white to pale yellow colour.

NLC based smart gels were prepared by varying the concentrations of Pluronic F-127 and Pluronic-68 using cold method technique. The polymer gel matrix of Pluronic F-127 (20-24% w/v) and Pluronic F-68 (2-6% w/v) was prepared and optimized by using 2-factor, 3-level full factorial design (3^2) using Design Expert® 9.0.3, which gave nine different run of the formulation. The polymers were directly dispersed gradually under stirring condition, within the NLC dispersion at 4 ºC until complete dissolution of the polymer to reaches final polymer concentration[32]. The addition of polymers in spite of preformed gel was the most significant step in the process, as it made the formulation process simple and abridged drug dilution in terms of mg/mL. The final concentration of MTX in the NLC based smart gel was 0.7 % (w/v).

3.2. Characterization of NLC

3.2.1. Particle size, Zeta potential measurement

The crucial factor in NLC performance is their particle size, because it significantly affects the rate and extent of drug release as well as drug absorption. The drug release is improved by smaller particle size; which offers larger interfacial area for drug diffusion. Nano size shows good transparency and increases surface area for partitioning of drug between oil and

water. The average particle size of NLC dispersion was found to be 107 nm ± 6 nm with a PDI of 0.365 ± 0.03 indicating uniformity in particle size distribution. The probability of Ostwald ripening was conquered due to narrow size distribution[41].

Various studies have reported that zeta potential plays an important role in the interaction of formulation with biological system[42, 43]. Zeta potential of the MTX-NLC dispersion was found to be -13.54 ± 1.1mV and increases with an increase in the surfactant concentration. This could be attributed to decrease in globule size; which leads to higher surface area and consequently higher zeta potential.

These results suggests that selected ratio of excipients favoured to form nanoemulsion; resulting in the formation of uniformly distributed nanosize NLC by modified method of hot homogenization followed by melt ultrasonication.

3.2.2. Scanning electron microscopy

The SEM microphotographs (Fig. 2) of obtained MTX-NLC dispersion depicted compact spherical shape, and particle diameters were in good agreement with DLS results. The mean diameter of NLC observed was around ~100 nm, devoid of any particle aggregation.

3.2.3. Entrapment efficiency and drug loading

Entrapment efficiency of the MTX-NLC dispersion was found to be 69.53% with 9% drug loading with respect to lipids. It reflects that 69.53 ± 1.23% of MTX is encapsulated in NLC system; however remaining amount of drug might be encapsulated in surfactant micelles in dispersion media. These results were in good agreement with earlier finding of Joshi *et al* [44]. Hence, the solubilized drug in the dispersion would be useful as loading dose, while drug entrapped in NLC will act as maintenance dose for prolonged release.

3.3. Characterization of MTX-NLC smart gel

Nine formulations of MTX-NLC based smart gel (F-1 to F-9) were prepared as per full factorial design by changing two independent variables, concentration of PF-127(A) and PF-68 (B) (Table 1). Table 2 shows the response values R1: Gelation temperature (°C); R2: Gelation time (sec); R3: Syringeability test (sec); R4: *In vitro* drug release studies (% Cumulative drug release) and were subjected to multiple regressions to yield polynomial equations, coefficient values indicate the effect by changing individual variable; 3D response surface graphs and contour plots were constructed.

3.3.1. Gelation temperature

The prepared MTX-NLC based smart gel exhibited temperature-dependent reversible sol-to-gel transition. When these systems were evaluated for gelation temperature studies, the smart gel systems transformed from sol-to-gel at a temperature less than body temperature. The formulation showed gelation temperature in range of 26.9 ± 0.65 ºC to 34.7 ± 0.33. Based on 3^2 factorial designs, the factor combinations of A and B resulted in different response variables for Gelation temperature (R1). The equation derived by best fit mathematical model to relate the response R1 and factors (A, B) was R1= +30.63333−2.66667A−1.43333B+0.1AB. ANOVA of the equation suggested the model F value 119.64, P value < 0.0001; indicating the model is significant. The increase or decrease effects of response on different level combination of independent variables are indicated by a positive or negative sign of the polynomial terms. As the predicted r^2 0.9587 is in reasonable concurrence with adjusted r^2 0.9780, the above polynomial equation showed a good fit of response variables at different levels. 3D surface plot of R1 is portrayed in Fig. 3A showed a significant decrease in gelation temperature with an increase in factors A and B.

The gelation temperature of the developed system was found to be concentration dependent; higher is the concentration of PF-127 and PF-68, higher is its thermoresponsivity. Though both Pluronics had substantial effect on sol-gel transition, PF-127 concentration was more significant to modify the gelation temperature. It was testified by Wei *et al*. that the gelation temperature of pluronic formulations mainly dependent on PF-127 concentration[45]. Vadnere *et al*. previously demonstrated greater hydrophilicity of Pluronic F68 than that of the Pluronic F127; interrupt the hydration shells around the hydrophobic portion of Pluronic F127 molecules[46]. Changes in Pluronic F127 molecule properties after a change in temperature and concentration in the Pluronic solution system was also described by Klouda *et al.*[47], which proved to be a major reason for selecting Pluronic F127 and Pluronic F68 for the study. Result of this, all formulations from the present study exhibited a rapid sol-to-gel transition at temperatures close to physiological temperature i.e., 37±0.5°C.

3.3.2. Gelation time

Being an injectable smart gel drug delivery system, along with the sol-gel transition at physiological conditions, another prerequisite is to form gel within an optimum time. Fast sol-gel transition is required to hold the smart gel and ultimately the drug at injection site so as to give a prolonged localized drug release. The results of gelation time indicated that prepared MTX-NLC based smart gel quickly responded to variation in gelation temperature. The formulations were subjected to their respective gelation temperatures; which resulted in quick gelation in less than 57 ± 1 sec. The gelation time of all the formulation was found within the range 41± 1 to 57± 1 sec. Based on 3^2 factorial designs, the factor combinations of A and B resulted in different response variables for gelation time (R2). The equation derived by best fit mathematical model to relate the response R2 and the independent variables was R2= +48.88889−4.33333A−

3.66667B+0.25AB. ANOVA of the equation suggested the model F value 247.13, P value < 0.0001 indicating that the model is significant. Also, the predicted r^2 0.9812 is in reasonable concurrence with adjusted r^2 0.9893. Gelation time was significantly influenced by the factors A and B. Increase in the polymers concentration led to decreased gelation time for around 20 sec. 3 Dimensional response (3D) plot of R2 is represented in Fig. 3B showed a significant decrease in gelation time with an increase in factors A and B. This might be due to increased viscosity of the system at an increasing level of factors A and B. Similar results were observed by Din *et al.* [48] during the development of novel solid lipid nanoparticle loaded thermosensitive hydrogel for rectal administration.

3.3.3. Syringeability test

Syringeability is important in clinical condition during administration of gel into the body using syringe and needle. Time taken to expel contents in the syringe by application of constant force is termed as syringeability time. The results of syringeability study indicated that prepared MTX-NLC based smart gel was easily syringeable through an 18 gauze needle. Syringeability time recorded for gel formulations was found within the range 8.12 ± 0.58 to 12.72 ± 0.43 sec. The equation derived for R3 by best fit mathematical model was R3= +10.45778 +1.163333A +1.023333B + 0.12AB with predicted r^2 0.8087 is in reasonable agreement with adjusted r^2 0.9388. The equation was found to be significant as the model F value found to be 41.88 and model P value was < 0.0006. The response surface plot for R3 (Fig. 3C) revealed significant linear increasing trend in syringeability time with an increase in factors A and B. This could be attributed to the fact that an increase in viscosity of the system, results in enhanced resistance to flow [48].

3.3.4. In vitro drug release study

In vitro drug release studies provide vital information about pretended performance of the formulation during *in vivo* conditions. The results of *in vitro* release studies indicated that drug release was prolonged. The equation derived for R4 by best fit mathematical model was: R4= 94.97 − 4.25833A − 1.40667B − 0.3375AB with predicted r^2 (0.8606) is in reasonable agreement with adjusted r^2 (0.9475). It was found that the effect of factor A is more significant than factor B; with an increase in factor A release rate of MTX from smart gels significantly decreased. Prolonged MTX release from formulations up to 120 h was mainly influenced by the factor A. In addition, the factor B has contributed for better performance of factor A in terms of quick gelation time and lower gelation temperature. ANOVA of the equation suggested the model F value 49.13, P value < 0.0004 indicating that the model is significant. Dimensional response (3D) plot of R4 is portrayed in Fig. 3D showed a significant decrease in drug release with an increase in A and B.

All formulations exhibited initial burst release followed by prolonged release of MTX. The initial burst release was due to unentrapped drug in the gel matrix in initial hours, followed by prolonged release of entrapped drug from the NLC core. Drug release from NLC is due to gradual degradation of the NLC spheres and concomitant diffusion of drug into the external polymer matrix. The conclusions drawn from the study were supported by the findings of Joshi *et al*[44]. The initial burst release of the drug followed by prolonged release is of great interest for the IA delivery of the drug. Initial burst release will provide the optimum concentration of the drug for immediate control of symptoms, followed by prolonged release which maintains the required concentration for overall treatment of RD[49].

3.3.5. Check point analysis and optimization of design

To optimize all the responses with different targets, a multi-criteria decision approach (a numerical optimization technique by the desirability function and a graphical optimization technique by the overlay plot) was used (Fig. 4). The optimized formulation (F-10) was obtained by applying constraints as R1=30 °C, R2 = 49 sec, R3=11 sec, R4= 90% on responses. These constrains were common for all the formulations. Recommended concentrations of the factors were calculated by the DoE from above plots which has highest desirability near to 1.0. The optimum values of selected variables obtained using DoE was 23.194 % of A and 2.604 % of B.

Desirability and overlay plot of DoE gave optimum values of both factors, from that final formulation was prepared. The optimized formulation (F-10) was prepared for check point analysis and evaluated for gelation time, gelation temperature, syringeability, *in v*itro drug release (% cumulative drug release) up to 108 h. The optimized formulation showed response variable as R1=29.6 ± 0.61 °C; R2= 49 ± 1 sec; R3= 10.68 ± 0.45 sec; R4 = 92.41 ± 6.79 %. There is a close agreement between predicted and observed values (Table 3) proved by desirability value of 0.8 with low relative errors (Fig. 5). It demonstrated the reliability of the optimization procedure followed in the present study to prepare formulation as per 3^2 factorial designs. Factors A and B with the composition of 23.2% and 2.6% are suitable for drug delivery as NLC based injectable smart gel, and thus chosen for MTX-NLC based smart gel delivery in this study.

Fig. 6 shows the *in vitro* release profile of MTX-NLC based smart gel sterilized using gamma irradiation. Our preliminary studies (data not shown) have indicated that gamma irradiation sterilization did not significantly affect release profiles of MTX. The release profile indicated that drug entrapped within the NLC core was not completely released even at the end of 8 h, and 92.41 % of drug release was obtained from the optimized formulation at 108 h. The

release data from NLC based smart gel was fitted into different models. The value of r^2 was found to be highest for the Higuchi model (r^2 = 0.98); which indicates that the test product follows matrix-diffusion-based release kinetics.

3.3.6. Drug content

The drug content of the optimized formulation was found to be 98.46% ± 0.32. The drug content value implied that the drug was significantly loaded in the smart gel formulations.

3.3.7. Viscosity studies

Viscosity of MTX-NLC based smart gel was measured at 8 ± 0.5°C and 37 ± 0.5°C representing the storage and the body temperature respectively. Viscosity studies of gel exhibited a temperature dependent increase in viscosity. This may be ascribed to the fact that pluronics, that are non-ionic poly propylene oxide triblock copolymers, get agglomerated into micelles at 37°C; which result from the polymer block dehydration with temperature. It has been portrayed that packing and micellar arrangement results in gel formation and at greater PF-127 concentrations, the gel is more entangled. Due to these micelle entanglements, they cannot be readily separated from each other, thereby causing rigidity and high viscosity of gel at higher pluronics concentrations [50, 51].

The viscosity of the optimized formulation was recorded low at 8 ± 0.5°C, however a significant increase in viscosity at 37 ± 0.5°C due to sol-gel conversion. The viscosity of MTX-NLC based smart gel at 8 °C was found to be 2085 cps, while a substantial increase in viscosity (69,522 cps) was observed at 37 °C.

3.4. Sterilization and sterility testing

To make it attractive in an increasing number of situations, it can be sterilized with gamma irradiation which offers various advantages like efficient, simple, convenient and

terminal treatment. Literature describes sterilization by radiation that comprises of a large diversity of disposable medical products, pharmaceuticals, implants and sutures, biological tissues and cosmetics[52].

Following gamma irradiation with a dose of 15.76 kGy, optimized formulation was rendered sterile. Only the non irradiated formulation, used as positive control, determined the clouding of the Mueller-Hinton broth in the sterility test, indicating that contamination of microorganisms was present.

3.5. *In vivo* study

On day 0, i.e., the treatment day, baseline (100%) knee swelling (mean ± S.D.) in MTX, MTX-NLC based smart gel and saline-treated rats was 3.43 ±0.27, 3.16 ± 0.44, 3.88 ± 0.28 mm, correspondingly. No noteworthy difference in knee swelling was observed between these groups. For control group, saline-treated rats were included in the study. Knee swelling records for MTX-NLC based smart gel treated rats were compared with MTX and saline treated rats to deduce whether intra-articular injection of MTX-NLC based smart gel will be able to alter the course of arthritis.

Fig. 7 depicted the effect of MTX, MTX-NLC based smart gel and saline treatment on right knee swelling. MTX-NLC based smart gel had more beneficial effect than free drug on knee swelling between day 1 and day 21. Conversely, 1 day after treatment, knee swelling (mean ± S.D.) in MTX-NLC based smart gel treated rats (74.3 ± 3.4 %; $P < 0.03$) was considerably reduced than in MTX treated rats (94.8 ± 2.4%). This variance persisted considerable all time to day 21 where knee swelling had reduced to 18.24 ±1.3% ($P < 0.004$) for MTX-NLC based smart gel treated rats and 77 ± 4.7% for MTX treated rats. The difference in

treating the complete Freund's adjuvant-induced arthritis in a Wistar rat model was related to their retention within the joint space.

The MTX-NLC based smart gel administered by an intra-articular route was effective in reducing inflammatory response, when compared to free MTX confirming the findings from previous literature[53]. Foong et al. reported liposome technology to preserve the efficacy of MTX when injected IA and it was found that liposomal MTX had stronger therapeutic effect than MTX alone[53,54]. Lipid nanoemulsion technology was also attempted to investigate anti-inflammatory action of MTX for IA treatment of RA. The study concluded that the association between lipid nanoemulsion and MTX presented a marked anti-inflammatory effect than that of IA commercial MTX treatment[55]. Development of MTX loaded hyaluronic acid as viscous emulsion and injected via IA route to form a drug depot was explored in another study by Son et al[56]. It was confirmed from the study that the enhanced RA repair was resulted from long-lasting drug release in articular joint. IA retention time can be improved by drug delivery systems while decreasing the toxicity level of the drug. The results of the current study confirmed these assumptions by demonstrating that, MTX-NLC based smart gel treated rat's knee swelling reduced gradually and nearly resumed to normal over the period of treatment. All these results depict that MTX incorporated into NLC based smart gel is desirable to show improved efficiency when compared to free MTX in conquering inflammation in RD.

3.6. Biocompatibility assessment

Knee inflammation was not seen in the animals as there were no macroscopic sign of joint stiffness, swelling or redness. The histology with haematoxylin and eosin staining of healthy rat joints injected with MTX-NLC based smart gel and saline-treated control joints was shown in Fig. 8. There was no inflammatory infiltration in the IA cavity. The MTX-NLC based

smart gel treated joint did not differ from the control joint. These results indicated that the formed smart gel demonstrate promising biocompatibility for the IA route of administration. Therefore, MTX-NLC based smart gel offers a nontoxic, biocompatible alternative for the effective management of arthritis.

4. CONCLUSIONS

Various concentrations of solid lipid and liquid lipid were used to prepare MTX-NLC based smart gels, by hot homogenization followed by melt ultrasonication. The NLC remained within the colloidal range and it was uniformly dispersed after suitably gelled by PF-127 and PF-68. The formulation displayed a sol-gel transition value which is lower than the body temperature. MTX-NLC based smart gel showed faster onset yet effecting a prolonged action as depicted from *in vitro* release. Moreover, developed smart gel was not toxic to the synovium, an indication of its biocompatibility. For establishing their efficacy in clinical use, these preclinical studies necessitate to be extrapolated to humans. In conclusion, the developed NLC based smart gel can have a dual advantage of biocompatibility and localised prolonged release. Thus, the study demonstrates that the developed smart gel has a great appeal for the convenient treatment of RD that may be explored in improving the limitations of existing drug delivery systems. We anticipate that there is a bright perspective on the future development of MTX-NLC based smart gel for localised and controlled drug delivery.

CONFLICT OF INTEREST

The author confirms that this article content has no conflict of interest.

ACKNOWLEDGEMENTS

The authors express gratitude to Indian Council for Medical Research (ICMR), New Delhi (IRIS ID: 2010-04380), for providing financial assistance. The authors are also grateful to JSS College of Pharmacy, JSS University for providing necessary facilities to carry out this research work.

REFERENCES

1. A. Chopra, *Rheum. Dis. Clin. North Am.*, 2000, **26**, 133-44.
2. S.J. Lee and A. Kavanaugh, *Best Pract. Res. Cl. Rh.*, 2003, **17**, 811-829.
3. N. Butoescu, O. Jordan and E. Doelker, *Eur. J. Pharm. Biopharm.*, 2009, **73**, 205-218.
4. C.G. Helmick, D.T. Felson, R.C. Lawrence, S. Gabriel, R. Hirsch, C.K. Kwoh, M.H. Liang, H.M. Kremers, M.D. Mayes, P.A. Merkel, S.R. Pillemer, J.D. Reveille and J.H. Stone, *Arthritis Rheum.* 2008, **58**, 15-25.
5. S.M. Seed, K.C. Dunican and A.M. Lynch, *Hosp. Pract.*, 2011, **39**, 62-73.
6. R.K. Studer and C.R. Chu, *J. Orthop. Res.*, 2005, **23**, 454–461.

7. C.G. Shinde, M.P. Venkatesh, T.P. Kumar and H.G. Shivakumar, *J. Pain Palliat. Care Pharmacother.,* 2014, **28**, 351-358.
8. A. Abou-Raya, S. Abou-Raya and T. Khadrawe, *Ann. Rheum. Dis.*, 2014, [Epub ahead of print]
9. C.Y. Wenham, A.J. Grainger, E.M. Hensor, A.R. Caperon, Z.R. Ash and P.G. Conaghan, *Rheumatology (Oxford).*, 2013, **52**, 888-92.
10. N. Varatharajan, I.G. Lim, A. Anandacoomarasamy, R. Russo, K. Byth, D.G. Spencer, N. Manolios and G.B. Howe, *Intern. Med. J.*, 2009, **39**, 228-236.
11. G. Mouterde, A. Baillet, C. Gaujoux-Viala, A. Cantagrel, D. Wendling, X. Le Loet and S. T. Chaeverbeke, *Joint Bone Spine*, 2011, **78,** 587-92.
12. C. Albert, O. Brocq, D. Gerard, C. Roux and L. Euller-Ziegler, *Joint Bone Spine,* 2006, **73**, 205–207.
13. J.P. Raynauld, C. Buckland-Wright, R. Ward, D. Choquette, B. Haraoui, J. Martel-Pelletier, I. Uthman, V. Khy, J. Tremblay, C. Bertrand and J. Martel-Pelletier, *Arthritis Rheum.,* 2003, **48**, 370–377.
14. R.G. Gray and N.L. Gottlieb, *Clin. Orthop. Relat. Res.,* 1983, **177**, 235-63.
15. G.V. Gordon and H.R. Schumacher, *J. Rheumatol*., 1978, **6**, 7-14.
16. M.H. Ellman and M.A. Becker, *Curr. Opin. Rheumatol*., 2006, **18**, 249-55.
17. T. Tosu, *J. Joint Surg.,* 1992, **11**, 87–95.
18. E. Horisawa, T. Hirota, S. Kawazoe, J. Yamada, H. Yamamoto, H. Takeuchi and Y. Kawashima, *Pharm. Res.*, 2002, **19**, 403-410.
19. R.H. Muller, M. Radtke and S.A. Wissing, *Adv. Drug Deliv. Rev.*, 2002, **54**, S131-S155.

20. F. Tamjidi, M. Shahedi, J. Varshosaz and A. Nasirpour, *Innov. Food Sci. Emerg*., 2013, **19**, 29-43.

21. S. Nie, W.L.W. Hsiao, W. Pan and Z. Yang, *Int. J. Nanomedicine*, 2011, **6**, 151-166.

22. T. Vohra, I. Kaur, H. Heer and R.R. Murthy, *Cancer Nanotechnol*., 2013, **4**, 1-12.

23. L.S. Liang, J. Jackson, W. Min, V. Risovic, K.M. Wasan and Burt H.M., *J. Pharm. Sci.*, 2004, **93**, 943-956.

24. S. Das and A. Chaudhury, *AAPS PharmSciTech*., 2011, **12**,(1): 62–76

25. I.R. Schmolka, *J. Biomed. Mater. Res*., 1972, **6**, 571-82.

26. X. Zhang, W. Pan, L. Gan, C. Zhu, Y. Gan and S. Nie, *Chem. Pharm. Bull.*, 2008, **56**, 1645-1650.

27. S.G. Lee, J.H. Jeong, S.R. Kim, K.M. Lee, B.K. Ahn, M.H. Kang and Y.W. Choi, *J. Pharm. Investig.*, 2012, **42**, 243-250.

28. B.S. Yannic, G. Robert and J. Olivier, *Eur. J. Pharm. Biopharm.*, 2008, **68**, 19-25.

29. E. Horisawa, T. Hirota, S. Kawazoe, J. Yamada, H. Yamamoto, H. Takeuchi and Y. Kawashima, *Pharm. Res.*, 2002, **19**, 403-410.

30. Y.K. Lin, Z.R. Huang, R.Z. Zhuo and J.Y. Fang, *Int. J. Nanomedicine*, 2010, **5**, 117-128.

31. A. Wakankar, Y. Chen, Y. Gokarn and F.S. Jacobson, *MAbs*., 2011, **3**, 161-172.

32. L. Ravani, E. Esposito, C. Bories, V.L. Moal, P.M. Loiseau, M. Djabourov, R. Cortesi and K. Bouchemal, *Int. J. Pharm.*, 2013, **454**, 695-702

33. R.A.M. Osmani, N.H. Aloorkar, D.J. Ingale, P.K. Kulkarni, U. Hani, R.R. Bhosale and D.J. Dev, *Saudi Pharm. J.*, 2015, **23**, 562-572.

34. T. Al Kayal, D. Panetta, B. Canciani, P. Losi, M. Tripodi, S. Burchielli, P. Ottoni, P.A. Salvadori and G. Soldani, *PLoS One*, 2015, **10**, e0125110.

35. U. Snekhalatha, M. Anburajan, B. Venkatraman and M. Menaka, *Z. Rheumatol.*, 2013, **72**, 375-382.

36. R.J. Griffiths, *Agents Actions*, 1992, **35**, 88-95.

37. H. Nomura, S. Takanashi, M. Tanaka, H. Haniu, K. Aoki, M. Okamoto and N. Saito, *Sci. Rep.*, 2015, **5**, 1-11.

38. B. Miao, C. Song and G. Ma, *J. Appl. Polym. Sci.*, 2011, **122**, 2139-2145.

39. R.P. Thatipamula, C.R. Palem, R. Gannu, S. Mudragada, and M.R. Yamsani, *Daru.,* 2011, 19, 23-32.

40. T.H. Tran, T. Ramasamy, D.H. Truong, H.G. Choi, C.S. Yong and J.O. Kim, *AAPS PharmSciTech*, 2014, **15**, 1509-1515.

41. V.D. Kumar, P.R.P. Verma and S.K. Singh, *LWT-Food Sci. Technol.*, 2015, **61**, 330-338.

42. S. Honary and F. Zahir, *Trop. J. Pharm. Res.,* 2013, **12**, 255-264.

43. S. Honary and F. Zahir, *Trop. J. Pharm. Res.,* 2013, **12**, 265-273.

44. M. Joshi, S. Pathak, S. Sharma and V. Patravale, *Int. J. Pharm.,* 2008, **364**, 119-126.

45. G. Wei, H. Xu, P.T. Ding, S.M. Li and J.M. Zheng, J. Control Release, 2002, **83**, 65–74.

46. M. Vadnere, G. Amidon, S. Lindenbaum and J.L. Haslam, *Int. J. Pharm.,* 1984, **22**, 207–218.

47. L. Klouda and A.G. Mikos, *Eur. J. Pharm. Biopharm.,* 2008, **68**, 34–45.

48. F.U. Din, O. Mustapha, D.W. Kim, R. Rashid, J.H. Park, J.Y. Choi, S.K. Ku, C.S. Yong, J.O. Kim and H.G. Choi, *Eur. J. Pharm. Biopharm.,* 2015, **94**, 64-72.

49. D. Dyondi, A. Sarkar and R. Banerjee, *J. Biomed. Nanotechnol.,* 2015, **11**, 1225-1235.

50. A. Cabana, A. Ait-Kadi and J. Juhasz, *J. Colloid Interface Sci.,* 1997, **190**, 307–312.

51. N. Jain, V. Aswal, P. Goyal and P. Bahadur, *J. Phys. Chem.,* 1998, **102**, 8452–8460.

52. J.W. Dorpema, *Radiat. Phys. Chem.*, 1990, **35**, 357-360.

53. W.C. Foong and K.L. Green, *J. Pharm. Pharmacol.,* 1993, **45**, 204–209.

54. W.C. Foong and K.L. Green, *J. Pharm. Pharmacol.,* 1988, **40,** 464–468.

55. S.B. Mello, E.R. Tavares, A. Bulgarelli, E. Bonfá and R.C. Maranhao, *Int. J. Nanomedicine.,* 2013, **8**, 443-449.

56. S. A. Reum, D.Y. Kim, P.S. Hun, J.J. Yong, K. Kim, K. B. Ju, Y.X. Yun, K.J. Ho, M.B. Hyun, H.D. Keun and K.M. Suk, *Sci. Rep.,* 2015, **5**, 14713.

List of Tables:

Table 1: Different combinations of NLC based smart gels using 3^2 factorial designs

Table 2: 3^2 factorial design layout and responses noted for MTX-NLC based smart gel

Table 3: Check point analysis of optimized formulations (F-10) of MTX-NLC based smart gel

Table 1: Different combinations of NLC based smart gels using 3^2 factorial designs

Formulation Code	Coded factor levels	
	A	B
F-1	−1	−1
F-2	0	−1
F-3	−1	1
F-4	1	−1
F-5	1	1
F-6	−1	0

F-7	0	0
F-8	0	1
F-9	1	0

Factors and their coded levels	−1	0	1
A: PF 127 amount (%)	20	22	24
B: PF 68 amount (%)	2	4	6

Table 2: 3^2 factorial design layout and responses noted for MTX-NLC based smart gel

Formulation Code	A	B	R1 (°C)*	R2 (sec)*	R3 (sec)*	R4 (%)*
F-1	−1	−1	34.7± 0.33	57± 1	8.12± 0.58	99.45±4.22
F-2	0	−1	32.4± 0.43	52± 1	9.72± 0.64	97.67±3.21
F-3	−1	1	31.8± 0.45	49± 2	10.24± 0.45	98.16±2.90
F-4	1	−1	29.4± 0.51	48± 2	10.12± 0.36	91.84±3.89

F-5	1	1	26.9± 0.65	41± 1	12.72± 0.43	89.20±4.11
F-6	−1	0	33.1± 0.64	54± 2	9.44± 0.51	99.17±5.62
F-7	0	0	30.9± 0.63	49± 1	10.68± 0.58	95.89±4.61
F-8	0	1	29.2± 0.27	45± 1	11.14± 0.47	93.16±3.91
F-9	1	0	27.3± 0.31	45± 1	11.94± 0.51	90.19±4.09

*Mean ± SD, n=3

Table 3: Check point analysis of optimized formulations (F-10) of MTX-NLC based smart gel

Formulation code	**A**	**B**	**R1 (°C)**	**R2 (sec)**	**R3 (sec)**	**R4 (%)**	**Desirability**
Predicted	23.194	2.604	30	48.76	10.38	93.55	0.833
Observed	23.2	2.6	29.6± 0.61	49± 1	10.68±0.45	92.41±6.79	-
Relative error	0.006	0.004	0.4	0.24	0.3	1.14	-
			Other evaluation parameters				
			Viscosity (cps)		**Drug content (%)**		

At 8°C	At 37°C	
2085	69522	98.46 ±0.32

List of Figures:

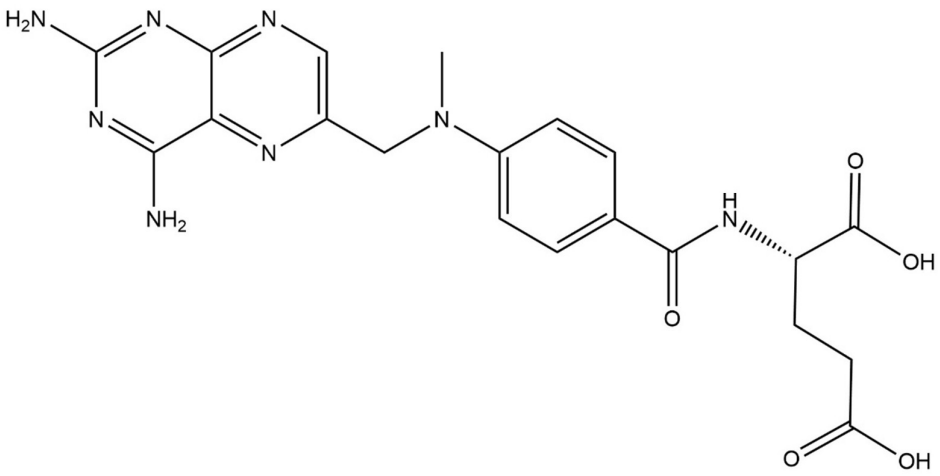

Fig 1. Chemical structure of Methotrexate

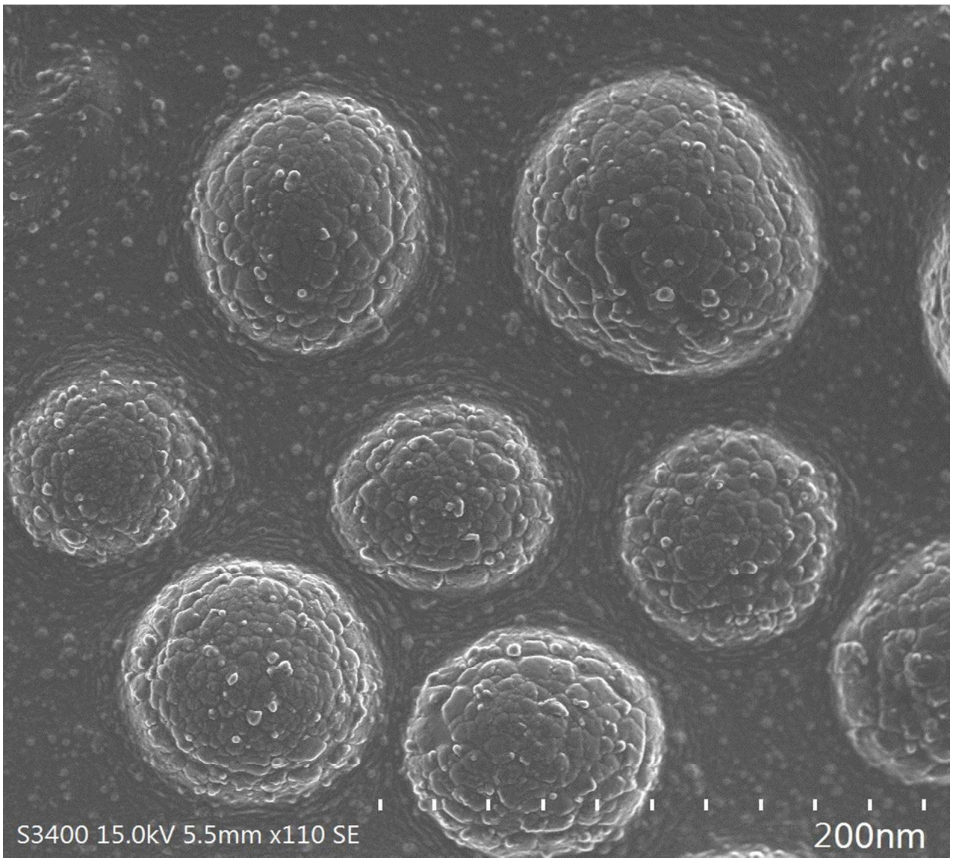

Fig 2. SEM Photomicrographs of optimized MTX loaded NLC

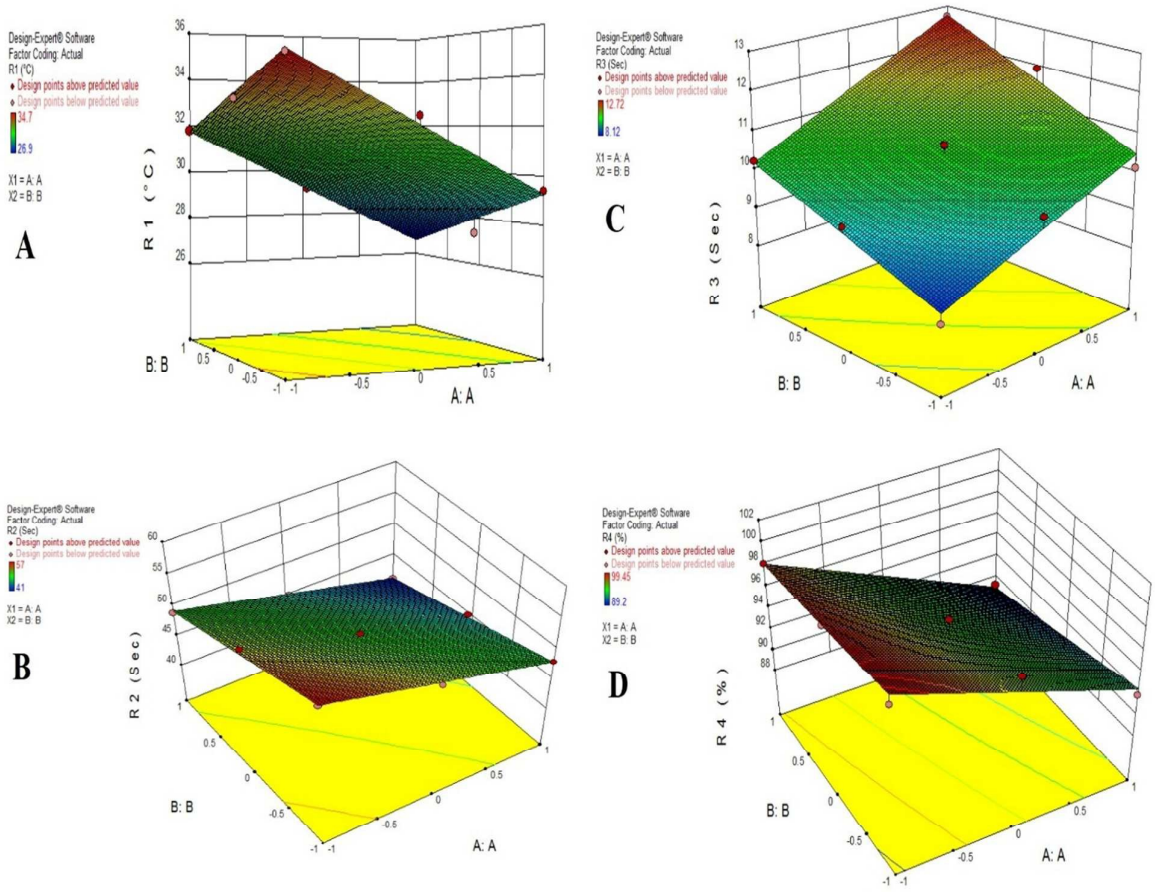

Fig 3. Response Surface Plot of (A) R1: Gelation temperature (°C); (B) R2: Gelation time (Sec); (C) R3: Syringeability test (sec) and (D) R4: *In vitro* drug release studies (% cumulative drug release) up to 108 h at different levels of A and B

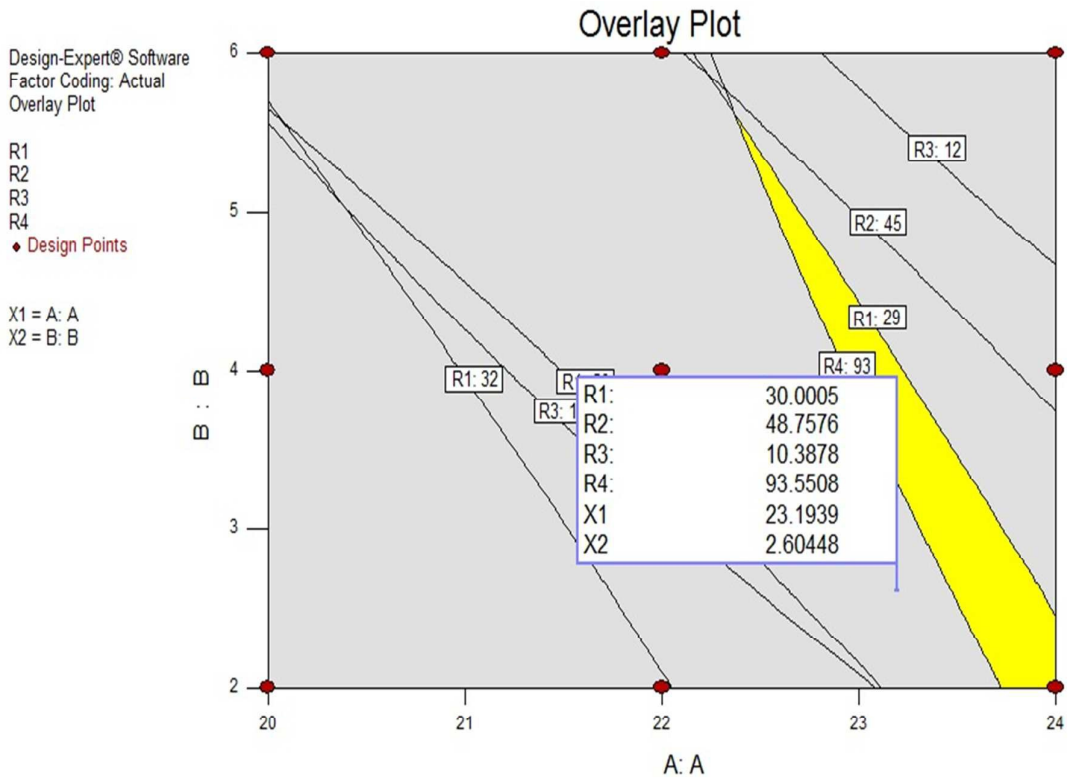

Fig 4. Overlay plot for optimization of MTX-NLC based smart gel

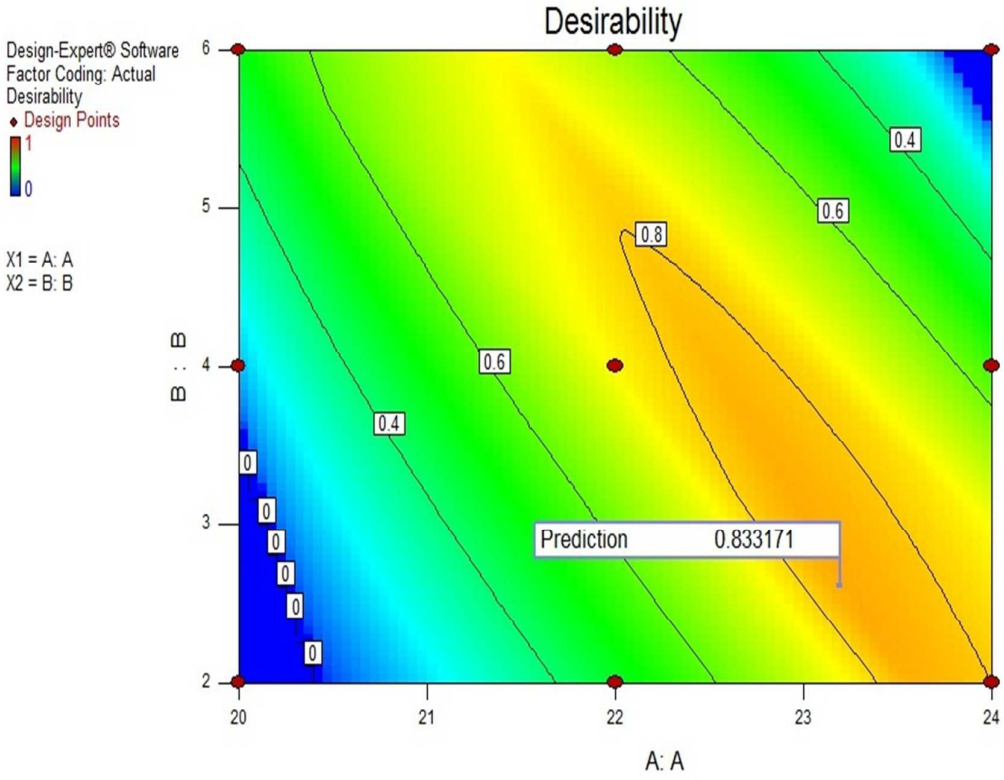

Fig 5. Contour plots represent overall desirability function of optimized formulation (F-10)

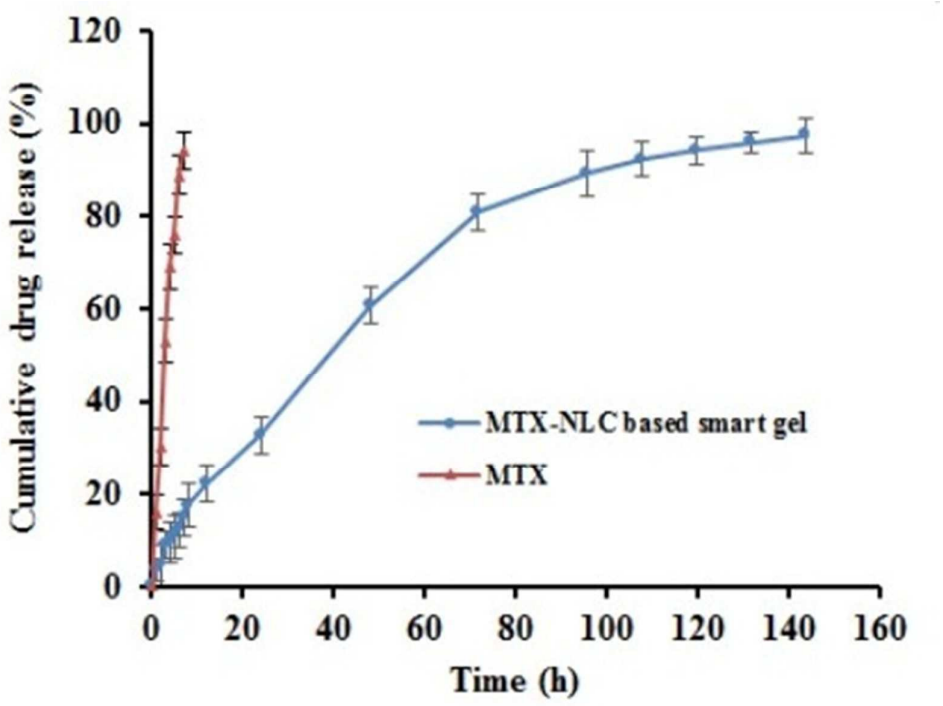

Fig 6. Comparative *In vitro* release profile of MTX and MTX-NLC based smart gel

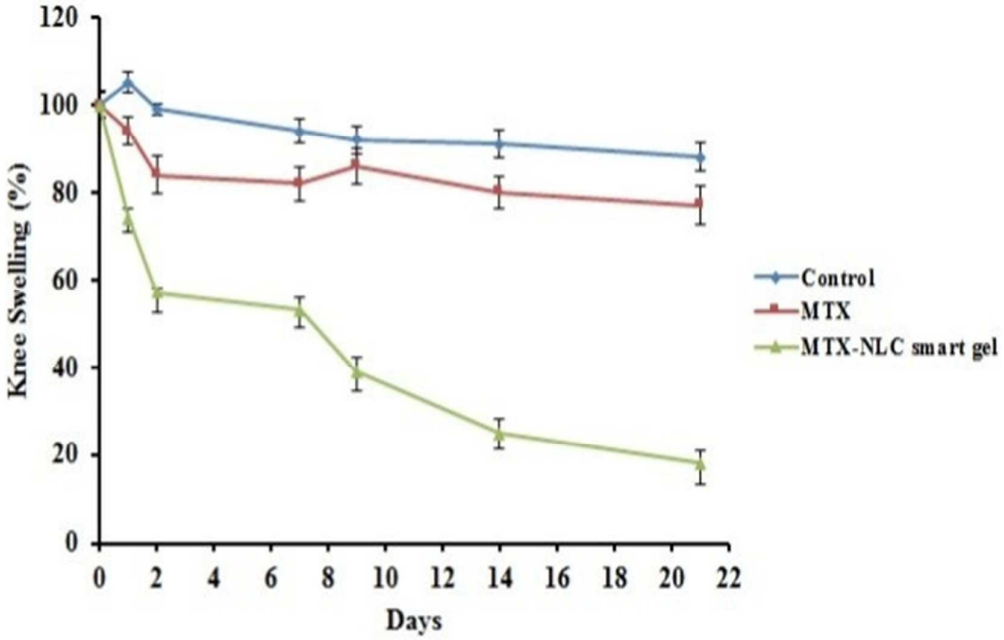

Fig 7. The anti-inflammatory effect of MTX and MTX-NLC based smart gel as assessed by a reduction in knee swelling in rats with adjuvant arthritis model. One day after treatment, knee swelling (mean ± S.D.) in MTX-NLC based smart gel treated rats was significantly less than MTX treated rats ($P < 0.03$)

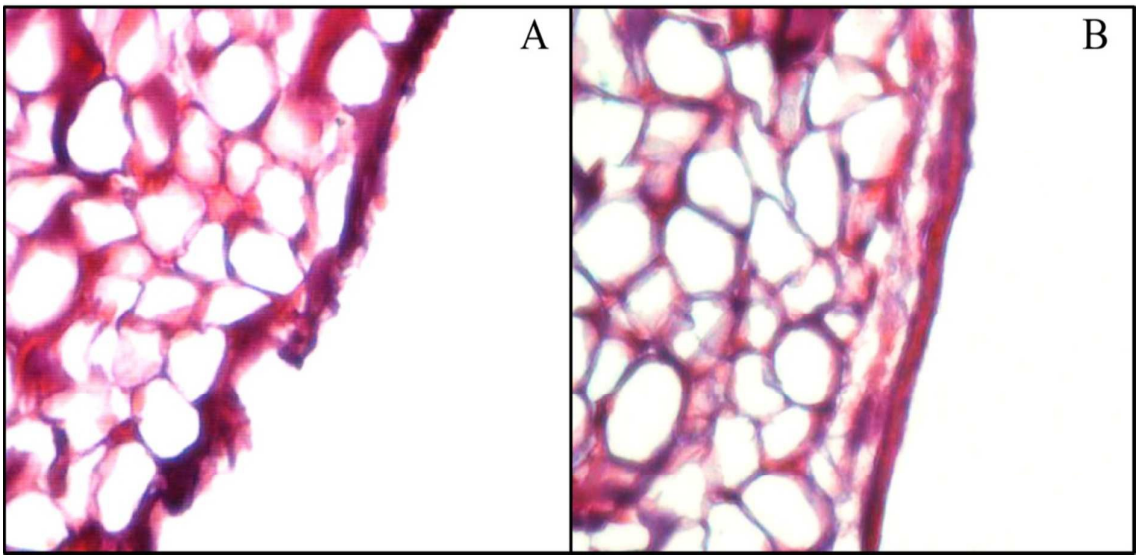

Fig 8. Representative H and E (hematoxylin and eosin) stained histological slides of synovial tissues from healthy rat knees after IA injection with (A) 100 µL of saline and (B) 100 µL of MTX-NLC based smart gel (magnification: X100)